Low-temperature cellulose hydrolysis to glucose in aqueous solutions over HY zeolite nanocrystals grafted on titania nanofibres

Longlong Shan, Jun Yan, Xinsheng Dong, Yang Wang, Xuebin Ke, Xingguang Zhang*

Address: College of Chemical Engineering, Nanjing Forestry University, No. 159 Longpan Road, Nanjing 210037, P.R. China. Corresponding author: x.g.zhang@hotmail.com

Abstract: In the past decades, renewable biomass has attracted attention as an alternative energy source for limited fossil fuels. As a huge amount of non-food biomass renewable energy source, the hydrolysis of cellulose to glucose by heterogeneous solid acids catalysts has caused increasing research interest. Herein we synthesized the zeolite HY nanocrystals grafted titania nanofibres (HY-TiO_2) with controlled crystal sizes, which could catalyze the hydrolysis of cellulose to glucose in aqueous solutions at relatively low temperatures (100-130°C). Characterization results XRD, TEM and FT-IR demonstrated that fine the zeolite HY nanocrystals and stable and well-distributed crystals (40-60 nm) on the surface of titania nanofibres. The HY-TiO_2 as a catalyst had better hydrolyze cellulose to glucose than the HYnano did under identical conditions. The results of characterized determined that the better hydrolysis performance of cellulose may due to the HY-TiO_2 catalyst does not aggregate and is more likely to dissolve and diffuse, thus enhancing the accessibility of the active site of the catalyst and the reactants.

Keywords: Cellulose, glucose, hydrolysis, diffusion, zeolite nanocrystals

Graphical Abstract

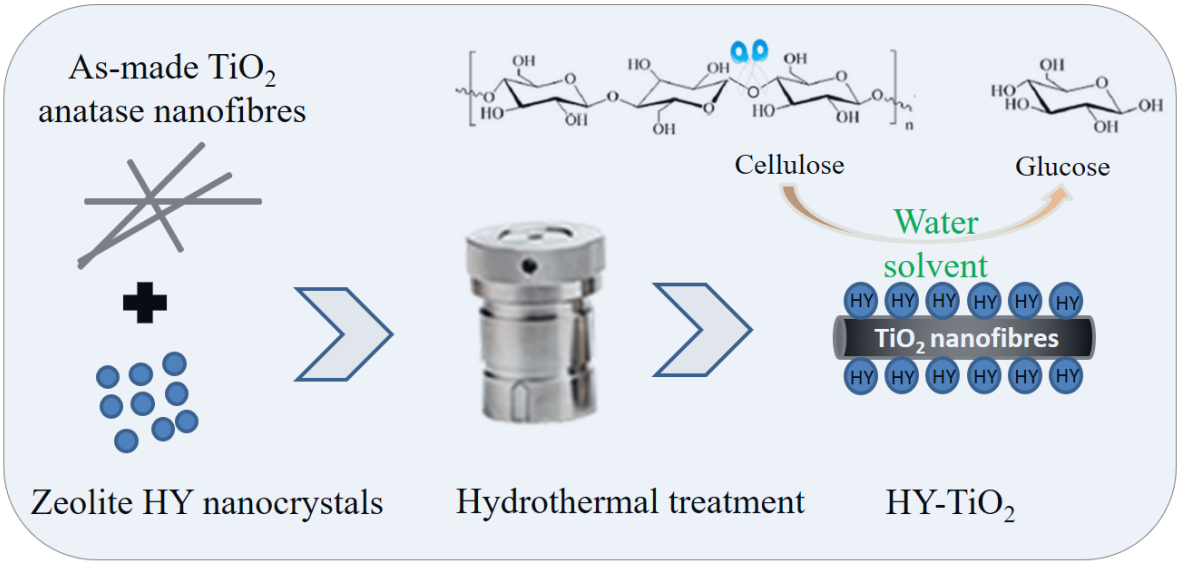

Essentials: Low-temperature cellulose hydrolysis to glucose in aqueous solutions over HY zeolite nanocrystals grafted on anatase nanofibres

1 Introduction

Today the world is short of energy, more and more people are paying attention to new energy resources. Everybody likes to pursue the goal that we can use clean fuels. Biomass is the fourth largest energy source after coal, oil and natural gas, and plays an important role in the entire energy system. Among various biomass resources, cellulose and hemicellulose account for about 60−80% of the total weight, which makes the development of its high-efficiency value-added catalytic process more and more important.[1-3] Cellulose is a huge amount of non-food biomass resources. And as a renewable energy source, the conversion of cellulose to fuels and chemicals has caused increasing research interest worldwide.[4,5] The direct and efficient hydrolysis of cellulose to glucose as the first step in cellulose conversion has received extensive attention using homogeneous catalysts or heterogeneous catalysts.[6,7] The catalytic hydrolysis of cellulose by homogeneous catalysts has been extensively studied, but its use has disadvantages, such as corrosion, environmental pollution, and difficulty in catalyst recovery.

In recent years, the homogeneous catalysts are replaced advantageously by heterogeneous solid acids catalysts, such as zeolites,[8,9] metal oxides,[10,11] polymeric catalysts,[12,13] magnetic catalysts,[14-16] and carbonaceous solid acids,[17,18] because heterogeneous catalysts are safe, easy separation, economic efficiency and environmental friendliness. In addition, heterogeneous catalysts often use ionic liquids as solvents for the hydrolysis reaction during the hydrolysis of cellulose to produce glucose. Due to the high viscosity of the ionic liquid, it is expensive and inconvenient to handle.[15,17,19,20] Due to the low solubility of cellulose in water and the large mass transfer resistance between cellulose and solid catalysts, the high yield of glucose from cellulose using heterogeneous catalysts remains a significant challenge. Whether it is a homogeneous catalyst or a heterogeneous catalyst, the cellulose hydrolysis reaction temperature generally exceeds 180 °C due to the strong

cellulose structure. Therefore, under mild reaction conditions, efficient hydrolysis of cellulose without any additives has become an urgent challenge.

In the field of zeolite porous materials, many efforts have been made to modify zeolites because small pores and agglomerated large particles of zeolite strongly hinder the diffusion of reactants, intermediates or products. For instance, introducing mesopores/macropores into zeolite framework through templating strategies has been demonstrated to make sense in many studies. Liu and coworkers' recent investigation on zeolite ZSM-5 single crystals with b-axis-aligned mesopores suggests that such oriented mesoporous materials exhibits an excellent hydrothermal stability and much higher catalytic activities in converting bulky substrates compared with conventional zeolite ZSM-5 with randomly oriented mesopores.[21,22] Inspired by these work, we design a new structure zeolite catalyst — zeolite nanocrystals supported on nanofibres substrates, hereby offer new opportunities. Since the high surface area and nanocrystals of zeolites can be exposed so as to alleviate the drawbacks of zeolite porous materials catalyst, the difficulty in separating and recycling catalyst solids, and more importantly the difficulty in synthesizing zeolite nanocrystals, because the zeolite nanocrystals are unable to move once grafted on the surface of the nanofibres substrate and thus coagulation during crystallization and calcination is prevented. And this new structure zeolite catalyst is active in hydrolysis of cellulose in the aqueous solutions at lower temperature.

2 Experimental Section

2.1 Materials

α-Cellulose (≤25μm), Anatase (99%, 325 mesh), Tetramethylammonium hydroxide solution (TMAOH, 10wt.% in H_2O), aluminium isopropoxide (≥98%), and Poly

(diallyldimethylammonium chloride) solution (PDDA, 20wt. % in water) were purchased from Aladdin Industrial Inc. (Shanghai, China). Colloidal silica(30wt. %) was purchased from Merck(Shanghai, China). Aqueous ammonia solution was purchased from Sinopharm Chemical Reagent Company. And NaY were purchased from the Catalyst Plant of Nankai University.

2.2 Catalyst Preparation

Synthesis of TiO_2 nanofibres. According to methods reported in the literature.[23] 3 g of anatase particles (~ 325 mesh from Aldrich) was mixed with 40 mL of 10 M NaOH. The suspension was sonicated for 0.5 h or stirred for 1.5 h until the solution become homogeneous. Transferred the solution into a 100mL autoclave with a PTFE container inside (around 2 /3 was filled). The autoclave was maintained at temperature of 180 ℃ for 48 h under static conditions. The precipitate (sodium-form anatase) was recovered, washed with distilled water to remove excessive NaOH, until the pH=7-9. It was ion-exchanged with H^+ (using 2000 mL of 0.1M HCl solution 3 times with stirring for 1h) to produce $H_2Ti_3O_7$; and washed again with distilled water until pH~7 was reached. It was washed with ethanol and then the $H_2Ti_3O_7$ nanofibers product was dried at 80℃ for 12 h. Finally, it was calcined at 700℃ for 5 h in a muffle furnace at a heating rate of 5℃/min.

Synthesis nanozeolite NaY colloidal solution. According to methods reported in the literature. [24]Clear zeolite Y precursor is prepared with molar composition of:1 Al_2O_3:4.35 SiO_2: 2.4 TMAOH: 0.048 Na_2O: 249 H_2O. Briefly, 25.5 g of H_2O, 17.4 g of TMAOH, 4.2 g of aluminium isopropoxide, and 8.7g of Colloidal silica (Ludox HS-30) were mixed with stirring for 2 days under room temperature. Then, the products are obtained by crystallization at 80, 100, 120, 140ºC for 3 days in the autoclaves. Finally, nanozeolite NaY seeds were obtained, (they were at the bottom of autoclaves) and stir the gel with a glass rod to make the

seeds disperse mainly in the mixture (No addition of anything).

Zeolite NaY grafted on $H_2Ti_3O_7$ nanofibres. According to methods reported in the literature.[25,26] Support treatment: $H_2Ti_3O_7$ nanofibres were immersed with aqueous ammonia solution with stirring for 1 h, and then separated by centrifugation/filtration, removed water. (Note: 28% NH_3-H_2O one drops, 60 mL water, diluted to pH=9.5-10.5; 1.0 g nanofibres and 60 ml diluted aqueous ammonium solution.) The NH_3-H_2O modified 1.0 g of $H_2Ti_3O_7$ nanofibres were modified with 1 M NaCl solution (60 mL, including 0.5wt% of PDDA together) for about 0.5 h with stirring, then centrifugation/filtration, removed the liquid solution. The residual PDDA was removed by redispersing the 1.0 g of $H_2Ti_3O_7$ nanofibres in aqueous ammonia solution 3 times (250ml = (200ml H_2O + 50ml 28% aqueous ammonium solution, 60 ml each) to centrifuge.

Graft zeolite seeds onto nanofibres: 1.0 *g* of nanofibres was added into the dilute synthesis solution (10 ml NaY seeds solution, 50 mL water). Stir the mixtures for 4 h continuously and then transfer the solutions into the autoclave reactor (100-ml autoclaves two for each sample). Crystallization was performed at 80, 100, 120, 140 ºC for 3 days. Thus obtained solid products were collected by centrifugation/filtration, final products were washed by water until the pH value reached 7-9, and dried at 80 ºC for 12 h. Then it was calcined at 550 ℃for 5 h in a muffle furnace at a heating rate of 5℃/min. The obtained catalysts (included pure nanozeolite NaY) were treated by typical ion-exchange of Na^+ with H^+ to form Brønsted acids according to methods reported in the literature,[27] and these catalysts were named as HYnano, HY-TiO_2-80, HY-TiO_2-100, HY-TiO_2-120, HY-TiO_2-140, respectively.

2.3 Characterization

The crystallinity of the catalysts were characterized by X-ray diffraction (XRD), using a Rigaku Smartlab with Cu Kα radiation (λ = 0.1542 nm) at a scan rate of 5°/min from 5 to 80

(2θ) at a voltage of 40 kV.

The morphology of the catalysts were examined by Field-emission scanning electron microscopy (FESEM) utilizing a JSM-7600F (JEOL Ltd., Japan) with an operating voltage of 30 kV. Transmission electron microscopy (TEM) images were obtained by a JEOL JEM-2100 instrument at the accelerating voltage of 200 kV.

The amount of acid sites was determined by Temperature-programmed desorption of ammonia (NH_3-TPD), using a AutoChem II 2920 apparatus. The sample (0.1g) was put into a U-tube reactor. The tube was initially purged with a He flow and heated to 350 °C for activation (30 mL/min, 1h). After the pretreatment, the sample was cooled to 100 °C and saturated with in 5% NH_3/He (30 mL/min, 1 h). Physically adsorbed ammonia was swept by purging a He flow of 40 mL/min for 0.5h. Finally, the packed bed was heated at a rate of 10 °C/min to 600 °C under the He flow.

Fourier transform infrared spectra (FT-IR) was used to detect the surface functional groups by a FTIR spectrophotometer (Thermo Electron Nicolet360, USA) using the KBr wafer technique 400–4000 cm^{-1}. Brönsted and Lewis acid density were determined by pyridine adsorption infrared (Py-FTIR) measurements using a Thermo Electron Nicolet360. Before test, the samples were prepared by grinding thoroughly with 0.12g KBr and visible samples to form self-supporting wafers. Then, they were placed in a sample cell coupled to a vacuum line and evacuated (10^{-3} Pa) in situ at 400 ^oC for 2 h to remove adsorbed water and other volatiles. After the temperature was cooled down to room temperature, drop 1~2 drops of pyridine to completely moisten/wet the sample wafers. After the adsorption was completed, the excessive pyridine was desorbed/removed under vacuum at 150 ^oC for 1h, and then the spectra were recorded.

2.4 Catalytic experiments

The performance of zeolite HY nanocrystals grafted titania nanofibres at different crystallization temperatures were tested in the process of hydrolysis of cellulose. Typically, 0.1 g catalyst and 0.2 g α-cellulose were placed into a 100 mL Teflon-lined stainless steel autoclave with 10 ml deionised water. Subsequently, after being heated to 130 °C, the reaction was started with stirring at a rate of 800 rpm for desired reaction times. After the reaction, the autoclave was cooled to room temperature. Afterwards, the products were filtered to separate the solid. The solid (catalyst and residual cellulose) was dried at 80 °C overnight and weighted to determine conversion of cellulose. The liquid phase were analyzed by High Performance Liquid Chromatography, the HPLC system (Agilent 1100) equipped with RI detector (Shimadzu RID-10A) and a Aminex HPX-87H column (Bio-Rad, 300 x 7.8 mm), using 5 mM H_2SO_4 as eluent with a flow rate of 0.5 mL min^{-1} at 50 °C.

The conversion of cellulose was calculated by weight difference in the solid before and after reaction basis on Equation (1).

$$Conversion\ (\%) = \frac{m_{starting\ cellulose} - \left(m_{recovered\ solid} - m_{catalyst}\right)}{m_{starting\ cellulose}} \times 100 \qquad (1)$$

The yield and selectivity of glucose was calculated basis on Equation (2) and Equation (3), respectively.

$$Yield\ (\%) = \frac{moles\ of\ glucose\ in\ product}{moles\ of\ cellulose\ loaded\ in\ the\ reaction\ (base\ on\ glucose\ unit)} \times 100 \qquad (2)$$

$$Selectivity\ (\%) = \frac{moles\ of\ glucose\ in\ product}{moles\ of\ cellulose\ converted\ (base\ on\ glucose\ unit)} \times 100 \qquad (3)$$

3 Results and Discussion

3.1 Structural features of the catalysts HY

Figure 1 (left) gave the X-ray powder diffraction patterns (XRD) of HY-TiO_2-80,

HY-TiO_2-100, HY-TiO_2-120 and HY-TiO_2-140 to identify the crystallographic phases of Y zeolite, as well as two reference samples of titania nanofibres and the bulk zeolite HY nanocrystals (HYnano). By comparison, we can find that one new peak (2θ=23° or 2θ=27.3°) are observed at HY-TiO_2-80, HY-TiO_2-100, HY-TiO_2-120 and HY-TiO_2-140, which is ascribed to the main characteristic peak of HY zeolite. But the new peak at HY-TiO_2-120 and HY-TiO_2-140 were weaker than that of at HY-TiO_2-80 and HY-TiO_2-100, because probably the zeolite HY nanocrystals do not crystallize as well on the titania nanofibres at 120°C and 140 °C. We can also see that the intensity of the diffraction peaks of HY-TiO_2-80, HY-TiO_2-100, HY-TiO_2-120 and HY-TiO_2-140 were significantly stronger than that of the titania nanofibres, indicating a higher crystallinity. Moreover, only one main peak appears indicates that the zeolite HY nanocrystals on titania nanofibres arranged in uniform orientation. [28]

In order to further demonstrate that the zeolite HY nanocrystals grafted on titania nanofibres, Fourier transform infrared spectra (FT-IR) was determined in **Figure 1 (right)**. We can see that the distinct bands at 475 cm^{-1} and 1092 cm^{-1}, ascribed to the bending modes and asymmetric stretching of Si–O–Si respectively,[29,30] were detected in the zeolite HY nanocrystals, HY-TiO_2-80, HY-TiO_2-100, HY-TiO_2-120 and HY-TiO_2-140. This spectrum also exhibits a weak band at 786 cm^{-1} ascribed to the symmetric stretching of Si–O–Si.[29,31] However, the bands of Si–O–Si of HY-TiO_2-120 and HY-TiO_2-140 were weaker than that in HY-TiO_2-80, HY-TiO_2-100. Typical peak of Ti–O was detected at about 946 cm^{-1} and 813 cm^{-1} in titania nanofibres, however, this peak was not detected in HY-TiO_2-80, HY-TiO_2-100, HY-TiO_2-120 and HY-TiO_2-140, because it may be overlapped by the strong band of the zeolite HY nanocrystals on the titania nanofibres.[30,31] Besides, The broad peak at 3450 cm^{-1} and 1629 cm^{-1} were assigned to the stretching vibration and bending vibration of O-H bond in absorbed water respectively,[32,33] while the weak peak at around 2924 cm^{-1} is probably

assigned to carbonaceous contaminants.[34] Hence, all these observations are consistent with the XRD results, indicating that the zeolite HY nanocrystals are well grafted onto the titania nanofibres.

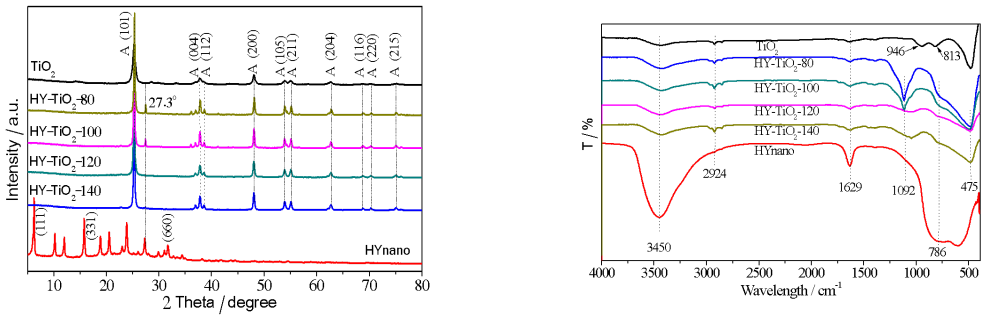

Figure 1. (Left) X-ray powder diffraction patterns (XRD); **(Right)** FT-IR spectra of the zeolite HY nanocrystals grafted on titania nanofibres at different crystallization temperatures, titania nanofibres, and the zeolite HY nanocrystals.

Figure 2 gave the images of transmission electron microscope (TEM). From these images we can see the morphology of the zeolite HY nanocrystals grafted on the titania nanofibres. The zeolite HY nanocrystals were stable and well-distributed (40-60 nm) on the surface of HY-TiO_2-80 and HY-TiO_2-100. However, the zeolite HY nanocrystals do not grow well on the surface of HY-TiO_2-120 and HY-TiO_2-140. After grafting the zeolite HY nanocrystals onto titania nanofibres, the spherical shape of HY nanocrystals (40-60 nm) was more uniform and diffused, as shown in **Figure S1**. This is consistent with the results of XRD and FT-IR, probably because of the crystallization of the zeolite HY nanocrystals seeds was affected as crystallization temperature increases. All these results suggest that we can achieve fine zeolite HY nanocrystals and stable and well-distributed crystals on the surface of titania nanofibres.

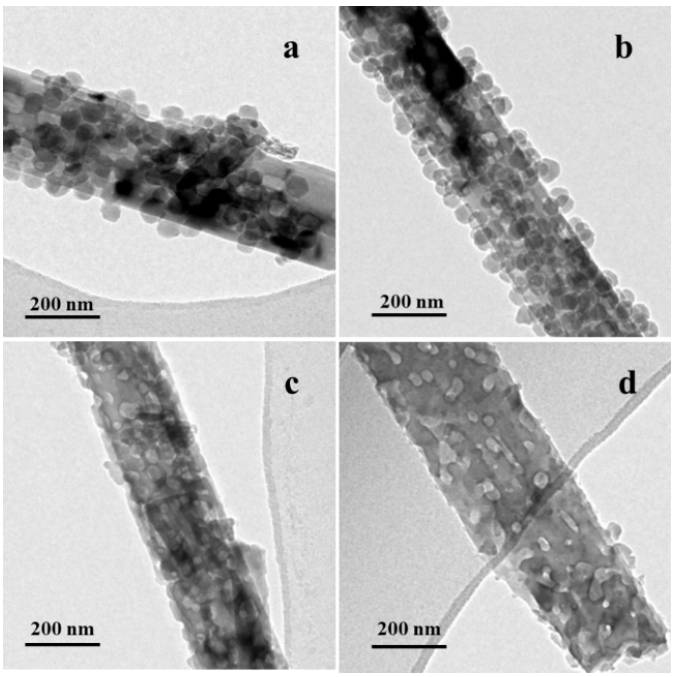

Figure 2. TEM images of zeolite HY nanocrystals grafted on titania nanofibres at different crystallization temperatures. (a) HY-TiO_2-80, (b) HY-TiO_2-100, (c) HY-TiO_2-120 and (d) HY-TiO_2-140.

3.2 Acid properties of the catalysts

Figure 3 (left) gave the NH_3-TPD spectra of titania nanofibres, the bulk zeolite HY nanocrystals (HYnano) and the zeolite HY nanocrystals grafted on titania nanofibres at different crystallization temperatures, and the quantitative results are showed in **Table S1**. In the low temperature range (100 – 250 °C), the peaks observed could be ascribed to the NH_3 desorption on the weak acid sites, whereas the peaks at high temperature range (400 –600 °C) could be ascribed to strong acid sites.[35] **Figure 3 (left)** show that the HYnano, HY-TiO_2-80, HY-TiO_2-100, HY-TiO_2-120 and HY-TiO_2-140 both had two absorption peaks around 200 °C and 460 °C, which were attributed to weak acid sites and strong acid sites, respectively. However, with an increase of the crystallization temperature, the absorption peak of the strong acid site was shifted to the weak acid site. By contrast, the total acid contents of the zeolite HY nanocrystals grafted on the titania nanofibres are less than that of the zeolite HY nanocrystals, as shown in **Table S1**. This indicated that acidity of HY-TiO_2-80, HY-TiO_2-100, HY-TiO_2-120 and HY-TiO_2-140 are weaker than that of the zeolite HY nanocrystals. In other

words, the bulk zeolite HY nanocrystals can provide more acid sites, in general which is beneficial to the improvement of catalytic performance.

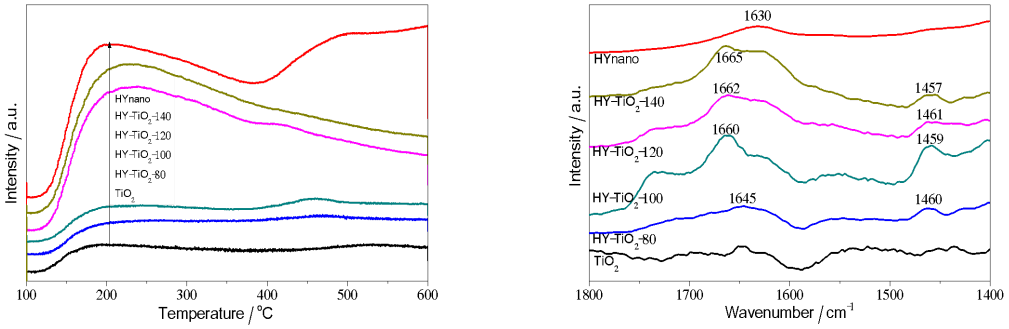

Figure 3. **(Left)** NH_3-TPD spectra and **(Right)** Py-FTIR spectra of titania nanofibres, the HYnano and the zeolite HY nanocrystals grafted on titania nanofibres at different crystallization temperatures.

In order to more insight into the types of acidic sites, the acidity of titania nanofibres, the bulk zeolite HY nanocrystals and zeolite HY nanocrystals grafted on titania nanofibres at different crystallization temperatures were identified by pyridine adsorption infrared (Py-FTIR) as show in **Figure 3 (right)**. According to reports that the band around at 1545 $cm^{-1}$and 1640 cm^{-1} correspond to pyridine adsorbed on the Brönsted acid sites, whereas the band around 1450 $cm^{-1}$and 1611 cm^{-1} are ascribed to pyridine adsorbed on Lewis acid sites.[36,37] We can see that only few irregular peaks were observed in titania nanofibres, indicating that there were hardly any acid sites. For the bulk zeolite HY nanocrystals, HY-TiO_2-80, HY-TiO_2-100, HY-TiO_2-120 and HY-TiO_2-140, the two absorption peaks around 1640 cm^{-1} and 1450 cm^{-1} were ascribed to pyridine adsorbed on the Brönsted acid sites and the Lewis acid sites respectively, indicated the presence of both Brönsted acid sites and Lewis acid sites.

In conclusion, from these results of NH_3-TPD and Py-FTIR we can find that the acidity of the bulk zeolite HY nanocrystals are stronger than that of the zeolite HY nanocrystals

grafted on titania nanofibres and all of these catalysts had Brönsted acid sites and Lewis acid sites. Nevertheless, the as-prepared catalysts had better hydrolysis performance on cellulose than that of the zeolite HY nanocrystals, which is indicated that the acidic sites of catalysts do not play a major role in cellulose hydrolysis, but the diffusion of catalysts dominates that.

3.3 Catalytic Performances

The performance of the as-prepared catalysts were investigated by hydrolysis experiments of cellulose, and compared with the bulk zeolite HY nanocrystals. As shown in **Figure 4 (left)**, the as-prepared catalysts had higher conversion of cellulose for the hydrolysis of cellulose than HYnano, and selectivity and yield of glucose was also higher than HYnano. Whereas the acidity of HYnano are stronger than that of the as-prepared catalysts and all of these catalysts had Brönsted acid sites and Lewis acid sites. These results indicated that the acidic sites of catalysts were not main factor affecting cellulose hydrolysis, but the diffusion of catalysts was the main fator, in this catalyst system. Since the zeolite HY nanocrystals grafted on titania nanofibres can hinder agglomerated of catalyst particles and enhance the diffusion of the catalyst, thus exposing more active sites increases its accessibility to β-1,4-glycosidic bonds of cellulose.

The catalytic performance of HY-TiO_2-80 and HY-TiO_2-100 were better than that of HY-TiO_2-120 and HY-TiO_2-140, which is ascribed to better zeolite HY nanocrystals and stable and well-distributed crystals on the surface of titania nanofibres at crystallization temperatures of 80°C and 100°C. In addition, HY-TiO_2-80 had the highest conversion of cellulose, combined with the characterization of the NH_3-TPD and Py-FTIR, which may be attributed to HY-TiO_2-80 having the most strong Lewis acid sites. Terminal reaction rate and terminal generation rate of cellulose hydrolysis are displayed in **Table S2**. It could be

discovered that the cellulose terminal reaction rates and the glucose terminal formation rates of HY-TiO_2-80 catalyst and HY-TiO_2-100 catalyst were similar, both of which were better than that of HYnano catalyst. These results also further indicated that the diffusion of catalyst is the main factor affecting the hydrolysis of cellulose.

Furthermore, we also studied the effect of ultrasonic pretreatment time of cellulose on the hydrolysis performance of cellulose by HYnano catalyst, results are shown in **Figure 4 (right)**. With the ultrasonic pretreatment time increases, the conversion of cellulose increases, and yield of glucose also increases except ultrasound pretreatment for 12 h, which may be attributed to the highest fructose yield at ultrasonic pretreatment 12h. These results are due to ultrasound swelling of cellulose, which increases the accessibility of catalyst acid sites to β-1,4-glycosidic bonds of cellulose. Therefore, it is also proved that the as-prepared catalyst has better diffusivity, which is beneficial to the active sites of the as-prepared catalyst and the reaction of the reactant. As shown in **Figure 5,** hydrolysis of cellobiose and sawdust were investigated by HYnano catalyst. We can find that the hydrolysis performance of HYnano catalyst on cellobiose was significantly higher than that on sawdust, which is attributed to the fact that sawdust are insoluble in water while cellobiose is soluble in water. So, the active sites of the catalyst are very accessible to the glycoside bond of cellobiose and reacts with it. Hence, this also can testify that the diffusion of the as-prepared catalyst increases the accessibility of the active site and the catalytic performance is high.

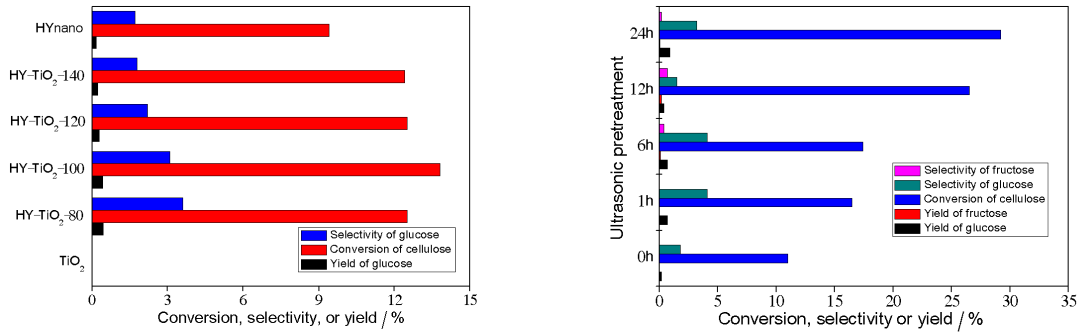

Figure 4. (Left) Conversion of cellulose, selectivity and yield of glucose for the hydrolysis of cellulose catalyzed by different catalysts. Reaction conditions: 0.2 g cellulose, 0.1 g catalyst, 10ml H_2O, reaction temperature 130℃, reaction time 72 h. **(Right)** Conversion of cellulose, selectivity and yield of glucose for the hydrolysis of cellulose treated by different ultrasonic pretreatment time (4 KHz, 45℃) over HYnano. ***Reaction condition*:** 0.2g cellulose, 0.1g HYnano, 10ml H_2O, reaction temperature 130℃, reaction time 24h.

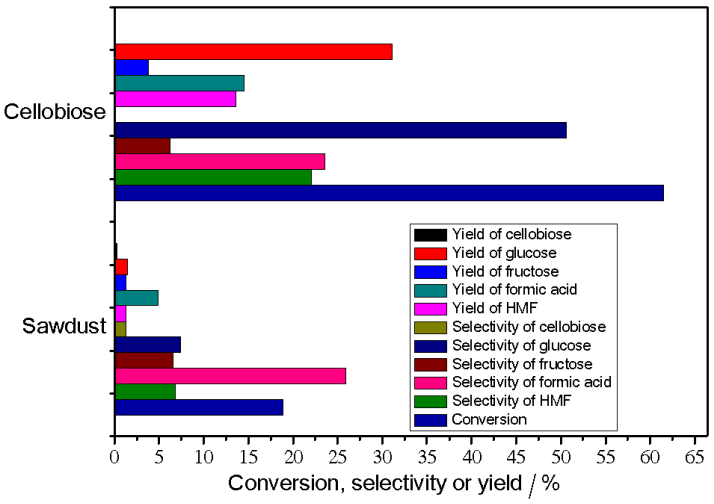

Figure 5. Hydrolysis effect of cellobiose and sawdust by HYnano catalyst. Reaction conditions: 0.2 g cellulose, 0.1 g catalyst, 10ml H_2O, reaction temperature 130℃, reaction time 24 h.

3.4 Mechanism discussion

It is well known that cellulose cannot dissolve in water, but water acts as a reaction substrate. Therefore, cellulose and solid acid catalysts are difficult to react in the

heterogeneous reaction, and solvent water plays a complex and critical role in cellulose hydrolysis reaction.[38] The reaction mechanism for cellulose hydrolysis in aqueous solutions is rarely reported. Base on the literature,[19,27,38] characterization results and experimental data, the reaction mechanism of hydrolysis of cellulose is proposed as shown in **Scheme 1**. First, the long chain of cellulose and the as-prepared catalysts were sufficiently contacted at 130ºC with agitation, since the HY nanocrystals are well dispersed on titania nanofibres and the as-prepared catalysts are not easily agglomerated. Subsequently, the Brönsted acid sites on the HY nanocrystals of as-prepared catalysts weakens the β-1,4-glycosidic bonds of cellulose, which is beneficial for water molecule to be inserted into the β-1,4-glycosidic bonds. And the Lewis acid sites can capture the hydroxyl group of the glucose monomer in the cellulose, which is beneficial to the weakening of the β-1,4-glycosidic bonds by Brönsted acid sites. Accordingly, the cellulose is hydrolyzed to glucose or other by-products.

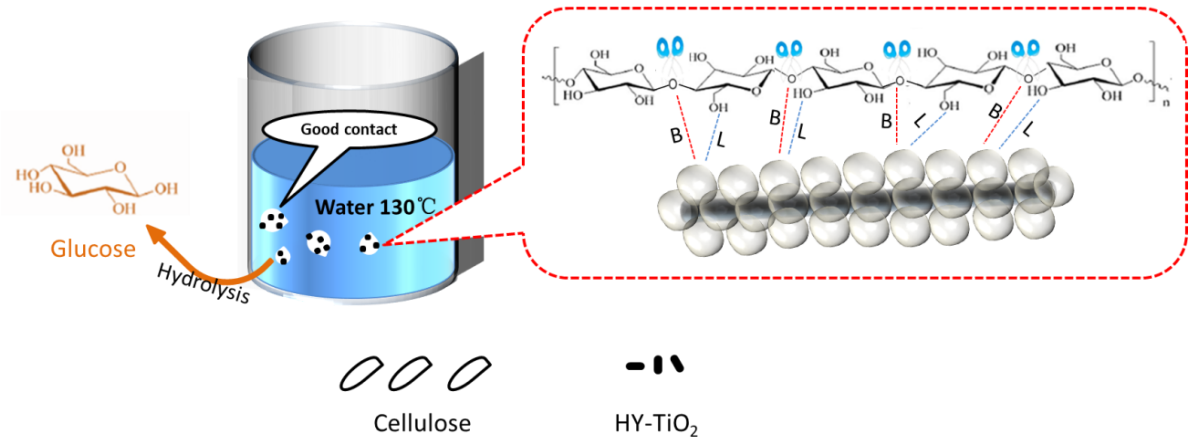

Scheme 1. Mechanisms of cellulose hydrolysis in aqueous solutions.

3.5 Reusability

To investigate the stability of as-prepared catalysts, the recycling of the HY-TiO_2-80 catalysts was conducted. After the first cellulose hydrolysis experiment, the remaining solids were washed three times with the distilled water and dried overnight at 80ºC. Then, the cellulose of the same mass as the first hydrolysis experiment was supplemented (the mass of

catalyst was considered not decreased), and the hydrolysis reaction was again carried out under the same conditions. The results indicate that the yield of glucose and the conversion of cellulose in the second hydrolysis experiment was 53% and 69% of that in the first hydrolysis experiment, respectively. The decrease in glucose yield and cellulose conversion may be due to the presence of hydrolytic residues that hinder some of the active sites of the catalyst and the loss of a large number of catalysts for recycling. As shown in **Figure S2**, we can see that all penetrating green beam of light in HYnano and a semi-penetrating green beam of light in HY-TiO_2-100 caused by the Tyndall effect. This indicated the HY-TiO_2-100 showed a good dispersibility in water.

4 Conclusion

In summary, the zeolite HY nanocrystals grafted on the titania nanofibres were synthesized and conducted hydrolysis of cellulose in aqueous solutions at lower temperature (130^{o}C). The zeolite HY nanocrystals grafted on the titania nanofibres had a better catalytic performance for cellulose hydrolysis than the bulk zeolite HY nanocrystals, which demonstrates its advantage not only in activating at low temperatures (130^{o}C), but also not easily agglomeration in nanocatalysts, more easily dissolved and diffused, on account of the zeolite HY nanocrystals grafted on titania nanofibres can expose more active sites and thus heighten its accessibility to β-1,4-glycosidic bonds of cellulose. Moreover, this study provides a new catalyst design approach to prevent nanocatalyst agglomeration and increase catalyst diffusivity.

Reference

1. Bodachivskyi I, Kuzhiumparambil U, Williams DBG. Acid-Catalyzed Conversion of Carbohydrates into Value-Added Small Molecules in Aqueous Media and Ionic Liquids. *Chemsuschem*. Feb 22 2018;11(4):642-660.

2. Liu QY, Zhang T, Liao YH, et al. Production of C-5/C-6 Sugar Alcohols by Hydrolytic Hydrogenation of Raw Lignocellulosic Biomass over Zr Based Solid Acids Combined with Ru/C. *Acs Sustain Chem Eng.* Jul 2017;5(7):5940-5950.

3. Zhang B, Chen B, Douthwaite M, et al. Macroporous-mesoporous carbon supported Ni catalysts for the conversion of cellulose to polyols. *Green Chem.* Aug 7 2018;20(15):3634-3642.

4. Johnson, Russell. Biofuels: Converting the biomasses. *Nature Chemistry.* 2012;5(1):5.

5. Shrotri A, Kobayashi H, Fukuoka A. Mechanochemical Synthesis of a Carboxylated Carbon Catalyst and Its Application in Cellulose Hydrolysis. *Chemcatchem.* Mar 18 2016;8(6):1059-1064.

6. Kobayashi H, Yabushita M, Komanoya T, Hara K, Fujita I, Fukuoka A. High-Yielding One-Pot Synthesis of Glucose from Cellulose Using Simple Activated Carbons and Trace Hydrochloric Acid. *Acs Catal.* Apr 2013;3(4):581-587.

7. Mu BN, Xu HL, Yang YQ. Accelerated hydrolysis of substituted cellulose for potential biofuel production: Kinetic study and modeling. *Bioresource Technol.* Nov 2015;196:332-338.

8. Karaki M, Karout A, Toufaily J, Rataboul F, Essayem N, Lebeau B. Synthesis and characterization of acidic ordered mesoporous organosilica SBA-15: Application to the hydrolysis of cellobiose and insight into the stability of the acidic functions. *J Catal.* Sep 2013;305:204-216.

9. Zhou LP, Liu Z, Bai YQ, Lu TL, Yang XM, Xu J. Hydrolysis of cellobiose catalyzed by zeolites-the role of acidity and micropore structure. *J Energy Chem.* Jan 2016;25(1):141-145.

10. Wang H, Guo YG, Chang CR, et al. Enhancing tungsten oxide/SBA-15 catalysts for hydrolysis of cellobiose through doping ZrO2. *Appl Catal a-Gen.* Aug 5 2016;523:182-192.

11. Zhang ZX, Sadakane M, Hiyoshi N, Yoshida A, Hara M, Ueda W. Acidic Ultrafine Tungsten Oxide Molecular Wires for Cellulosic Biomass Conversion. *Angew Chem Int Edit.* Aug 22 2016;55(35):10234-10238.

12. Onda A, Onda S, Koike M, Yanagisawa K, Tsubaki S, Hiraoka M. Catalytic Hydrolysis of Polysaccharides Derived from Fast-Growing Green Macroalgae. *Chemcatchem.* Jul 24 2017;9(14):2638-2641.

13. Yang Q, Pan XJ. Bifunctional Porous Polymers Bearing Boronic and Sulfonic Acids for Hydrolysis of Cellulose. *Acs Sustain Chem Eng.* Sep 2016;4(9):4824-4830.

14. Guo HX, Lian YF, Yan LL, Qi XH, Smith RL. Cellulose-derived superparamagnetic carbonaceous solid acid catalyst for cellulose hydrolysis in an ionic liquid or aqueous reaction system. *Green Chem.* 2013;15(8):2167-2174.

15. Xiong Y, Zhang ZH, Wang X, Liu B, Lin JT. Hydrolysis of cellulose in ionic liquids catalyzed by a magnetically-recoverable solid acid catalyst. *Chem Eng J.* Jan 1 2014;235:349-355.

16. Yamaguchi D, Watanabe K, Fukumi S. Hydrolysis of Cellulose by a Mesoporous Carbon-Fe-2(SO4)(3)/gamma-Fe2O3 Nanoparticle-Based Solid Acid Catalyst. *Sci Rep-Uk.* Feb 9 2016;6.

17. Chung PW, Yabushita M, To AT, et al. Long-Chain Glucan Adsorption and Depolymerization in Zeolite-Templated Carbon Catalysts. *Acs Catal.* Nov 2015;5(11):6422-6425.

18. Shen F, Smith RL, Li LY, Yan LL, Qi XH. Eco-friendly Method for Efficient Conversion of Cellulose into Levulinic Acid in Pure Water with Cellulase-Mimetic Solid Acid Catalyst. *Acs Sustain Chem Eng.* Mar 2017;5(3):2421-2427.

19. Wang JY, Zhou MD, Yuan YG, Zhang Q, Fang XC, Zang SL. Hydrolysis of cellulose catalyzed by quaternary ammonium perrhenates in 1-allyl-3-methylimidazolium chloride. *Bioresource Technol.* Dec 2015;197:42-47.

20. Yuan YG, Wang JY, Fu NH, Zang SL. Hydrolysis of cellulose in 1-allyl-3-methylimidazolium chloride catalyzed by methyltrioxorhenium. *Catal Commun.* Feb 10 2016;76:46-49.

21. Liu FJ, Willhammar T, Wang L, et al. ZSM-5 Zeolite Single Crystals with b-Axis-Aligned Mesoporous Channels as an Efficient Catalyst for Conversion of Bulky Organic Molecules. *J Am Chem Soc.* Mar 14 2012;134(10):4557-4560.

22. Zecevic J, Gommes CJ, Friedrich H, de Jongh PE, de Jong KP. Mesoporosity of Zeolite Y: Quantitative Three-Dimensional Study by Image Analysis of Electron Tomograms. *Angew Chem Int Edit.* 2012;51(17):4213-4217.

23. Zhang XG, Ke XB, Zheng ZF, Liu HW, Zhu HY. TiO2 nanofibers of different crystal phases for transesterification of alcohols with dimethyl carbonate. *Appl Catal B-Environ.* May 5 2014;150:330-337.

24. Holmberg BA, Wang HT, Norbeck JM, Yan YS. Controlling size and yield of zeolite Y nanocrystals using tetramethylammonium bromide. *Micropor Mesopor Mat.* Apr 18 2003;59(1):13-28.

25. Ke XB, Zhang XG, Liu HW, Xue S, Zhu HY. Efficient catalysts of zeolite nanocrystals grown with a preferred orientation on nanofibers. *Chem Commun.* 2013;49(84):9866-9868.

26. Yuranov I, Renken A, Kiwi-Minsker L. Zeolite/sintered metal fibers composites as effective

structured catalysts. *Appl Catal a-Gen.* Mar 18 2005;281(1-2):55-60.

27. Yu J, Wang JY, Wang Z, Zhou MD, Wang HY. Hydrolysis of cellulose promoted by silicalite-1 modified HY zeolite in 1-ethyl-3-methylimidazolium chloride. *Cellulose.* Mar 2018;25(3):1607-1615.

28. Kulak A, Lee Y-J, Park YS, Yoon KB. Orientation-Controlled Monolayer Assembly of Zeolite Crystals on Glass and Mica by Covalent Linkage of Surface-Bound Epoxide and Amine Groups. *Angewandte Chemie.*

29. Pakdel E, Daoud WA. Self-cleaning cotton functionalized with TiO2/SiO2: Focus on the role of silica. *J Colloid Interf Sci.* Jul 1 2013;401:1-7.

30. Zhang X, Zhang F, Chan KY. Synthesis of titania-silica mixed oxide mesoporous materials, characterization and photocatalytic properties. *Appl Catal a-Gen.* Apr 28 2005;284(1-2):193-198.

31. Landi S, Carneiro J, Ferdov S, et al. Photocatalytic degradation of Rhodamine B dye by cotton textile coated with SiO2-TiO2 and SiO2-TiO2-HY composites. *J Photoch Photobio A.* Sep 1 2017;346:60-69.

32. Kuźniarska-Biernacka I, Parpot P, Oliveira C, et al. Norbornene Oxidation by Chiral Complexes Encapsulated in NaY Zeolite. *The Journal of Physical Chemistry C.* 2014;118(33):19042-19050.

33. Chung NH, Dien LQ, Cuong TD, Van Lieu N, Hoang PH. Influence of the acidity of solid catalyst HSO3-ZSM-5 on the hydrolysis of pretreated corncob. *RSC Advances.* 2018;8(73):41776-41781.

34. Zhou G, Jiang L, He D. Nanoparticulate Ru on TiO2 exposed the {1 0 0} facets: Support facet effect on selective hydrogenation of benzene to cyclohexene. *J Catal.* 2019;369:352-362.

35. Condon JB. *Surface Area and Porosity Determinations by Physisorption*2006.

36. Cai Y, Xu XF, Wang H, et al. Bifunctional Co/Al-SBA-15 Catalyst with Tunable Acidity for Selective Production of Aviation Fuel. *Ind Eng Chem Res.* Mar 21 2018;57(11):3844-3854.

37. Liu F, Wang TF, Zheng YY, Wang JF. Synergistic effect of Bronsted and Lewis acid sites for the synthesis of polyoxymethylene dimethyl ethers over highly efficient SO42-/TiO2 catalysts. *J Catal.* Nov 2017;355:17-25.

38. Cai HL, Li CZ, Wang AQ, Xu GL, Zhang T. Zeolite-promoted hydrolysis of cellulose in ionic liquid, insight into the mutual behavior of zeolite, cellulose and ionic liquid. *Appl Catal B-Environ.* Jul 23 2012;123:333-338.

Supporting Information

Low-temperature cellulose hydrolysis to glucose in aqueous solutions by HY zeolite nanocrystals grafted on titania nanofibres

Longlong Shan, Jun Yan, Xinsheng Dong, Yang Wang, Xingguang Zhang*

Address: College of Chemical Engineering, Nanjing Forestry University, No. 159 Longpan Road, Nanjing 210037, P.R. China. Corresponding author: x.g.zhang@hotmail.com

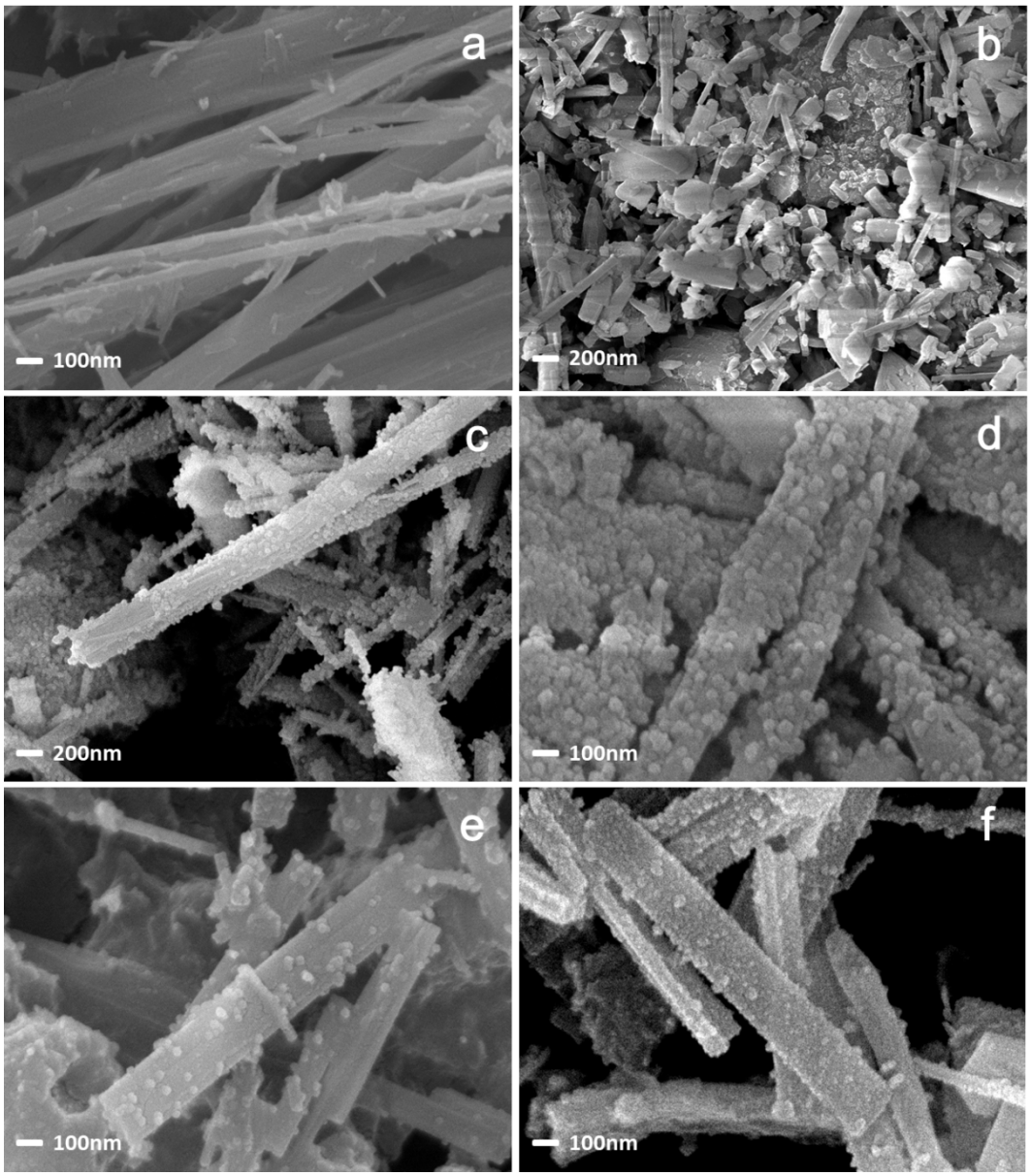

Figure S1. SEM images of (a) titania nanofibres, (b) HYnano, (c) HY-TiO_2-80, (d) HY-TiO_2-100, (e) HY-TiO_2-120 and (f) HY-TiO_2-140.

Table S1. Quantitative analysis of NH_3-TPD profiles.

Catalysts	Desorption peak temperature/^{o}C		Amount of acid sites/ mmol g^{-1}		Total amount of acid sites/ mmol g^{-1}
	low	high	weak	strong	
TiO_2	196	530	0.035	0.020	0.055
HYcom	190	588	0.188	0.166	0.354
HY-TiO_2-80	225	470	0.029	0.023	0.052
HY-TiO_2-100	216	458	0.034	0.027	0.061

HY-TiO_2-120	228	--	0.477	--	0.477
HY-TiO_2-140	227	--	0.472	--	0.472

Table S2. Terminal reaction rate and terminal generation rate.

Catalysts	Terminal reaction rate		Terminal generation rate	
	r_r [a](mol)	r_r [b] (g)	r_g [c] (mol)	r_g [d] (g)
HYcom	5.6 x 10^{-5}	3.39	9.5 x 10^{-7}	0.06
HY-TiO_2-80	6.6 x 10^{-5}	29.14	2.5 x 10^{-6}	1.09
HY-TiO_2-100	7.5 x 10^{-5}	27.87	2.4 x 10^{-6}	0.88
HY-TiO_2-120	--	3.18	--	0.07
HY-TiO_2-140	--	3.15	--	0.06

[a]moles of cellulose converted divided by the ratio of the total acid amount of the catalyst to the strong acid amount.

[b]moles of cellulose converted divided by the total acid amount of the catalyst.

[c]moles of glucose in product divided by the ratio of the total acid amount of the catalyst to the strong acid amount.

[d]moles of glucose in product divided by the total acid amount of the catalyst.

Reaction conditions: 0.2 g cellulose, 0.1 g catalyst, 10ml H_2O, reaction temperature 130℃, reaction time 72 h.

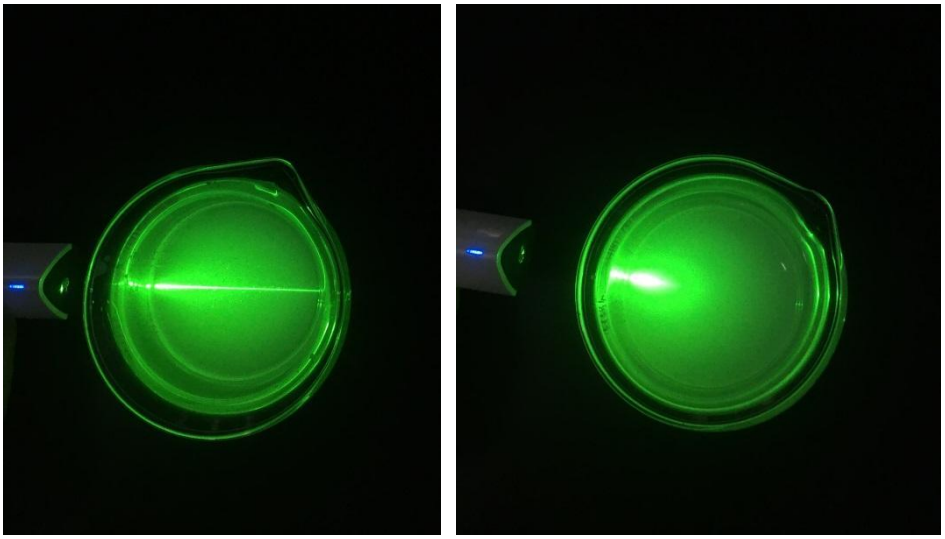

Figure S2. Pictures of **(Left)** HYnano and **(Right)** HY-TiO_2-100 Sufficient dispersed in aqueous solutions after standing for 22h.